THE JOURNAL OF BIOLOGICAL CHEMISTRY VOL. 286, NO. 32, pp. 28544–28555, August 12, 2011

Dynamic Modification of Sphingomyelin in Lipid Microdomains Controls Development of Obesity, Fatty Liver, and Type 2 Diabetes*[S]

Received for publication, April 28, 2011, and in revised form, June 10, 2011 Published, JBC Papers in Press, June 13, 2011, DOI 10.1074/jbc.M111.255646

Susumu Mitsutake[‡1], Kota Zama[‡], Hazuki Yokota[‡], Tetsuya Yoshida[§], Miki Tanaka[§], Masaru Mitsui[§], Masahito Ikawa[¶], Masaru Okabe[¶], Yoshikazu Tanaka[§], Tadashi Yamashita[‖], Hiroshi Takemoto[§], Toshiro Okazaki[**], Ken Watanabe[‡‡], and Yasuyuki Igarashi[‡]

From the Departments of [‡]Biomembrane and Biofunctional Chemistry and [‖]Developmental Biotechnology, Faculty of Advanced Life Science, Hokkaido University, Sapporo 001-0021, the [§]Shionogi Innovation Center for Drug Discovery, Shionogi and Co., Limited, Sapporo 001-0021, the [¶]Research Institute for Microbial Diseases and Pharmaceutical Sciences, Osaka University, Osaka 565-0871, the [**]Department of Clinical Laboratory, Medicine/Hematology, Faculty of Medicine, Tottori University, Tottori 683-8503, and the [‡‡]Department of Bone and Joint Disease, National Center for Geriatrics and Geriatrics and Gerontology, Aichi 474-8511, Japan

Lipid microdomains or caveolae, small invaginations of plasma membrane, have emerged as important elements for lipid uptake and glucose homeostasis. Sphingomyelin (SM) is one of the major phospholipids of the lipid microdomains. In this study, we investigated the physiological function of sphingomyelin synthase 2 (SMS2) using SMS2 knock-out mice, and we found that SMS2 deficiency prevents high fat diet-induced obesity and insulin resistance. Interestingly, in the liver of SMS2 knock-out mice, large and mature lipid droplets were scarcely observed. Treatment with siRNA for SMS2 also decreased the large lipid droplets in HepG2 cells. Additionally, the siRNA of SMS2 decreased the accumulation of triglyceride in liver of leptin-deficient (*ob/ob*) mice, strongly suggesting that SMS2 is involved in lipid droplet formation. Furthermore, we found that SMS2 exists in lipid microdomains and partially associates with the fatty acid transporter CD36/FAT and with caveolin 1, a scaffolding protein of caveolae. Because CD36/FAT and caveolin 1 exist in lipid microdomains and are coordinately involved in lipid droplet formation, SMS2 is implicated in the modulation of the SM in lipid microdomains, resulting in the regulation of CD36/FAT and caveolae. Here, we established new cell lines, in which we can completely distinguish SMS2 activity from SMS1 activity, and we demonstrated that SMS2 could convert ceramide produced in the outer leaflet of the plasma membrane into SM. Our findings demonstrate the novel and dynamic regulation of lipid microdomains via conformational changes in lipids on the plasma membrane by SMS2, which is responsible for obesity and type 2 diabetes.

Obesity and insulin resistance are commonly associated with nonalcoholic fatty liver disease, leading to nonalcoholic steatohepatitis. Elucidation of the mechanisms underlying fat accumulation in liver is a very important matter.

Studies have revealed that the biological membrane contains regions known as lipid microdomains that are enriched in sphingolipids, glycosphingolipid, or cholesterol. There are many types of microdomains, differing in lipid composition or detergent solubility, and each microdomain might have a distinct function, such as acting as a "raft" or "glycosynapse" (1–3). Caveolae are small invaginations on the plasma membrane and are sites with many glycosphingolipid, sphingomyelin, and cholesterol-rich lipid microdomains. Mice deficient in caveolin 1, a scaffolding protein of caveolae, are lean and resistant to diet-induced obesity, suggesting that caveolae and lipid microdomains may be important for the uptake of triglycerides (TG)[2] and fatty acids (4). Both caveolae and lipid microdomains are now emerging as active centers for metabolism, with implications in obesity, diabetes, and other metabolic disorders (5).

Along with cholesterol, sphingomyelin (SM) is a major component in lipid microdomains. Its synthetic enzyme is sphingomyelin synthase (SMS), for which the gene was identified in 2004 (6, 7). This enzyme has three isoforms, SMS1, SMS2, and SMSr. SMS1 is responsible for the bulk of SM production in the Golgi apparatus, and SMSr controls ceramide homeostasis in the endoplasmic reticulum, regulating the synthesis of ceramide phosphoethanolamine (8, 9). In a recent report, SMS2 deficiency attenuated NFκB activation and decreased atherosclerosis (10–12). However, the study did not fully address the mechanism of SMS2 involvement in atherosclerosis and NFκB activation or whether SMS2 has a function distinct from SMS1. The SMS2 deficiency might also affect the metabolism of ceramide, sphingosine, and sphingosine 1-phosphate. Because these bioactive lipids act in signal transduction (13, 14), their

* This work was supported by a Future Drug Discovery and Medical Care Innovation Program from the Ministry of Education, Culture, Sports, Science and Technology of Japan.

[S] The on-line version of this article (available at http://www.jbc.org) contains supplemental Table S1.

[1] To whom correspondence should be addressed: Kita 21, Nishi 11, Kita-ku, Sapporo 001-0021, Japan. Tel./Fax: 81-11-706-9047; E-mail: susumu-m@pharm.hokudai.ac.jp.

[2] The abbreviations used are: TG, triglyceride; SM, sphingomyelin; FA, fatty acid; DIO, diet-induced obesity; HFD, high fat diet; ND, normal diet; GTT, glucose tolerance test; WAT, white adipose tissue; oxLDL, oxidized LDL; PPAR, peroxisome proliferator activated receptor; DIM, detergent-insoluble membrane microdomain; SNALP, stable nucleic acid lipid particle; FAT, fatty acid transporter; SMase, sphingomyelinase; MβCD, methyl-β-cyclodextrin; MEF, mouse embryonic fibroblast; pAb, polyclonal antibody; PC, phosphatidylcholine; Cer, ceramide.

effects could be complex requiring additional studies to elucidate mechanisms.

In this study, we reveal that SMS2 is responsible for diet-induced obesity and lipid droplet formations in liver. We further provide details implicating SMS2 as a novel regulator of lipid microdomain structure and function.

EXPERIMENTAL PROCEDURES

Generation of SMS2 KO Mice and Animal Studies—A vector for targeting deletion of the SMS2-exon 2, containing a cassette encoding β-galactosidase and a neomycin-selectable marker (Nls-lacZ and PGK-neo), was electroporated into mouse D3 embryonic stem cells. Homologous recombinations were selected using G418 and Southern blotting.

Recombinant cells were karyotyped to ensure that 2N chromosomes were present in most metaphase spreads. Chimeric mice derived from correctly targeted ES cells were mated with C57BL/6 mice to obtain F1 *Sgms2*$^{+/-}$ mice. The recombination event was also confirmed by LA-PCR using tail samples of the mice obtained from *Sgms2*$^{+/-}$ × *Sgms2*$^{+/-}$ mating (Fig. 1*B*). PCR primers used to the LA-PCR were as follows: *a*, 5′-CCAAGTGACCTTCAAGTTTTGCTGTCTC-3′; *b*, 5′-CCAAGTGACCTTCAAGTTTTGCTGTCTC-3′; *c*, 5′-CAGGGTTTTCCCAGTCACGACGTTG-3′; *d*, 5′-TACATGATGTGTGATGACTACATGCCAG-3′; *e*, 5′-TCGCCTTCTATCGCCTTCTTGAC-3′; and *f*, 5′-GCATGCGTTCAGCGCGTTTGTATCCAC-3′. The primer positions are illustrated in Fig. 1*A*. All experiments were performed using N8 generation, which was obtained by eight rounds of backcrossing to C57BL/6 (*B6.129-sgms2*^{tm1Kenw}). The generation of SMS1 knock-out mice has described previously (15). Leptin-deficient *ob/ob* mice were obtained from Japan SLC Inc. (Hamamatsu, Japan).

To establish diet-induced obesity, the mice were fed a high fat diet (60% kcal from fat; 58Y1, TestDiet, Richmond, IN) from weeks 4 to 15 of age. Control mice were fed a standard chow diet (AIN76A, TestDiet) during the same period. Body weight was measured once a week. The amount of food intake was monitored during weeks 7–9.

The amounts of triglycerides, free fatty acids, and cholesterol in plasma and liver tissues were determined using a Triglyceride E-test Wako kit (Wako, Japan), a NEFA C-test Wako kit (Wako), and a Cholesterol E-test Wako kit (Wako), respectively. The isolated liver from each mouse was fixed with 4% paraformaldehyde, and 8-μm-thick frozen sections were prepared as described previously (16). The sections were stained with standard hematoxylin and eosin, and lipid droplets were stained with Oil-Red-O as described elsewhere (17).

Glucose Tolerance Test (GTT)—Following a 16-h fast, mice were injected intraperitoneally with a glucose solution (2 g/kg body weight). Glucose levels in blood collected from the tail vein before and after glucose injection (at 15, 30, 60, and 120 min) were measured using an ACCU-CHEK Aviva glucometer (Roche Applied Science). Plasma insulin levels in 8-week-old male mice were determined by a mouse insulin ELISA kit (Shibayagi, Gunma, Japan).

Real Time PCR—Using a combination of TRIzol® and PureLink™ RNA mini kits (Invitrogen), total RNA was extracted from the liver and adipose tissue of WT and SMS2 KO mice, according to kit instructions. First strand cDNA was synthesized using a PrimeScript RT master mix (TAKARA Bio, Otsu, Japan), and then real time PCR was performed using selected primers (supplemental Table 1) by SYBR Premix EX Taq (TAKARA Bio) and a Thermal Cycler Dice Real Time System (TAKARA Bio) following the manufacturer's instructions. Transcript levels were normalized to glyceraldehyde-3-phosphate dehydrogenase (GAPDH) or hypoxanthine-guanine phosphoribosyltransferase in liver or adipose tissue, respectively.

Quantification of SM, Cer, and PC—SM and Cer amounts in isolated tissue or cells were determined using electron ionization-LC/MS (LC, Agilent1100, Agilent Technologies; MS, LCQ fleet, ThermoFisher Scientific), as described previously (18–20). The amount of PC was determined using a phosphatidylcholine assay kit (BioVision). We used Cer (C16:0, d18:1) and SM (C16:0, d18:1) as standards to quantify Cer and SM, respectively. Standards were obtained from Avanti Polar Lipid (Alabaster, AL).

SDS-PAGE and Western Blotting—SDS-PAGE and Western blotting were performed according to the standard methods of Laemmli (21) and Towbin *et al.* (22), respectively. For protein detection on Western blot, we employed an anti-V5 monoclonal antibody (mAb) (Sigma), anti-V5 polyclonal antibody (pAb) (Sigma), anti-FLAG mAb (Sigma), anti-FLAG pAb (Sigma), anti-calnexin pAb (Abcam, Cambridge, MA), anti-caveolin 1 mAb (BD Biosciences), or anti-CD36 mAb (eBioscience, San Diego) as a primary antibody, and an anti-mouse IgG-HRP antibody (GE Healthcare), anti-rabbit IgG-HRP antibody (GE Healthcare), or anti-rat IgG-HRP antibody (GE Healthcare) as a secondary antibody. Bands were detected using a combination of an ECL Plus kit (GE Healthcare) and luminescent image analysis by an LAS4000 (Fuji Film, Tokyo). For CD36 detection in liver tissue, de-*N*-glycosidase (New England Biolabs, Beverly, MA) was added to samples prior to performing SDS-PAGE.

Preparation and Co-Immunoprecipitation Analysis of Detergent-insoluble Lipid Microdomains—COS7 cells were co-transfected with plasmids using Lipofectamine 2000 (Invitrogen) according to the manufacturer's instructions, and then the cells were incubated overnight. To isolate detergent-insoluble lipid microdomains, the cells were lysed, homogenized, and subjected to a sucrose density gradient according to the method described previously (23). In brief, the cells were incubated on ice with chilled lysis buffer containing 20 mM CHAPS (Sigma), Complete™ protease inhibitor mixture (Roche Applied Science), and PhoStop™ phosphatase inhibitor mixture (Roche Applied Science) in TNE buffer (10 mM Tris-HCl buffer, pH 7.5, 150 mM NaCl, 5 mM EDTA). The resulting lysate was adjusted to 42% sucrose and overlaid with a discontinuous sucrose gradient (6 ml of 30% sucrose or 2 ml of 0% sucrose) in TNE buffer. The tube was centrifuged at 34,100 rpm for 18 h in an SW41 rotor (Beckman Instruments), and the solution was fractionated from the top to the bottom. For co-immunoprecipitation experiments, the cells were lysed with lysis buffer containing 1% Brij 99 (Sigma) and Complete™ and PhoStop™ inhibitor mixtures (Roche Applied Science) in TNE buffer, and then the lysates were incubated with anti-FLAG M2 beads (Sigma) at

4 °C for 4 h. The beads were then washed four times with lysis buffer and subjected to SDS-PAGE.

siRNA Experiments and Quantification of Lipid Droplet Formation—HepG2 cells were grown in 6-well plates and transiently transfected with siRNA (h-siSMS2-1, 5′-GGGCAUUGCCUUCAUAUAU-3′; h-siSMS2-2, 5′-GCACACGAACACUACACUA-3′; control siRNA, 5′-UUCUCCGAACGUGUCACGU-3′) using Lipofectamine™ RNAiMAX (Invitrogen) according to the manufacturer's instructions. After 2 days, the formation of lipid droplets was induced by adding oleic acid/BSA mixture; final oleic acid concentration was 400 μM in culture media. After a 1-day incubation, the cells were fixed with 4% paraformaldehyde, and the lipid droplets were stained with Nile Red. The size and number of the lipid droplets were quantified using a fluorescent microscope (BZ-9000, Keyence, Osaka, Japan). *In vivo* siRNA experiments were performed as described previously using an siRNA delivery system of stable nucleic acid lipid particles (SNALP) (24). In brief, a SNALP/siRNA mixture containing SMS2 siRNA (m-siSMS2-1, 5′-GGCUCUUUCUGCGUUACAA-3′; m-siSMS2-2, 5′-GGAUGGUAUUGGUUGGGUU-3′; or control siRNA, 5′-UUCUCCGAACGUGUCACGU-3′) was administered intravenously into the tail vein of leptin-deficient *ob/ob* mice in a total volume of 10 ml/kg. After 10 days, the triglycerol amount in the liver of each mouse was determined.

Generation of SM-reconstituted Cells—The generation and analysis of SMS1 knock-out mice have been described previously (15). We generated double knock-out mice lacking both SMS1 and SMS2 and isolated mouse embryonic fibroblasts (MEF) from the mouse embryo. The MEF were immortalized by SV40 T antigen as described previously (25). From the immortalized MEF, we cloned the cell line ZS2. V5-tagged SMS1 and SMS2 were stably expressed in ZS2 cells by retrovirus gene transfer systems (Clontech) using the pQCXIP-SMS1-V5 and pQCXIH-SMS2 vector, respectively, according to the manufacturer's instructions. The obtained cells, which stably expressed SMS1 or SMS2, were named ZS2/SMS1 and ZS2/SMS2, respectively. We also immortalized MEF from SMS2 knock-out mice (SMS2 KO-MEF) and control littermate WT mice (WT-MEF). Additionally, reconstituted cells (SMS2 KO/SMS2 MEF) were produced using a retrovirus gene transfer systems with the pQCXIH-SMS2 vector as above. Cells were maintained in a humidified chamber with a 5% CO_2 atmosphere and cultured in Dulbecco's modified Eagle's medium (DMEM, Sigma) supplemented with 10% FBS. When we determined SM levels, the cells were cultured with the serum-free medium OptiPro SFM (Invitrogen) to block the SM supply from serum.

Metabolic Labeling of SM and Analysis of Sphingomyelin Synthase Activity—The *in vitro* SM synthase activity of cells was determined by BODIPY-C5-Cer, as described previously (26). Experiments using the CERT inhibitor HPA-12 were performed as described by Yasuda *et al.* (27). For the recovery experiment of SM, cells were labeled with [^{14}C]choline for 5 h and preincubated for 30 min with 80 μM dynasore (a dynamin II inhibitor; Sigma) in DMEM containing 10% FBS. The medium was changed to DMEM containing 100 microunits/ ml bacterial SMase (*Staphylococcus aureus*, Sigma) and 80 μM dynasore, and the cells were incubated for 30 min. The cells were then washed twice with DMEM, and incubated for 60 min in DMEM containing 80 μM dynasore. In each step, lipids were extracted and separated on a Silica Gel 60 thin layer chromatography plate (Merck) as described previously (6). Bands corresponding to [^{14}C]SM were quantified by imaging analyzer FLA7000 (Fuji film).

Uptake Assay for [^{14}C]Oleic Acid—Uptake assays utilizing [^{14}C]oleic acid (American Radiolabeled Chemicals, St. Louis) were performed as described previously (28).

Fluorescence Imaging—A pcDNA6.2-GFP-SMS2, pHcRed-CD36/FAT, or pHcRed-caveolin 1 plasmid was co-transfected to COS7 cells using Lipofectamine™2000 (Invitrogen) according to the manufacturer's instructions. After an overnight incubation at 37 °C, fluorescent images were directly obtained by a confocal laser scanning microscope, FluoView®FV10i (Olympus, Tokyo). For immunofluorescent microscopy, ZS2/SMS1 or ZS2/SMS2 cells were fixed and then permeabilized for 10 min in phosphate-buffered saline with 4% paraformaldehyde and 0.2% Triton X-100. The cells were incubated at room temperature for 4 h with both an anti-V5 mAb (Invitrogen) and an anti-GM130 pAb (BD Biosciences) and then for 2 h with Alexa 488-conjugated anti-mouse IgG (Invitrogen) or Alexa 594-conjugated phalloidin (Invitrogen). Coverslips were mounted with Prolong Gold®antifade with DAPI (Invitrogen), and confocal images were obtained using the FluoView®FV10i microscope.

Plasmid Construction—All plasmids used in this study were made using the Gateway® recombination system (Invitrogen). The cDNA of SMS1, SMS2, CD36/FAT, or caveolin 1 was amplified from mouse liver cDNA (Clontech) by PCR with selected primers as follows: SMS1, 5′-CACCATGTTGTCTGCCAGGACCATG-3′ and 5′-TGTGTCGTTTACCAGCCGG-3′ (the stop codon was disrupted for C-terminal protein fusion); SMS2, 5′-CACCATGGATATCATAGAGACAGCAAAA-3′ and 5′-GGTAGACTTCTCATTATCCTCCC-3′ (the stop codon was disrupted for C-terminal protein fusion); CD36/FAT, 5′-CACCATGGGCTGTGATCGGAACTGTG-3′ and either 5′-TTATTTTCCATTCTTGGATTTGCAAGCAC-3′ or 5′-TTTTCCATTCTTGGATTTGCAAGCAC-3′ (the stop codon was disrupted for C-terminal protein fusion); and CAV1, 5′-CACCATGTCTGGGGGCAAATACGTAG-3′ and 5′-TCATATCTCTTTCTGCGTGCTGAT-3′. The cDNA was then cloned to a pENTR™D-TOPO vector (Invitrogen). As a destination vector, we employed a pcDNA6.2/V5-DEST or pcDNA6.2/C-EmGFP-DEST vector (Invitrogen). The pQCXIP (Clontech), pQCXIH (Clontech), pHcRed (Clontech), and p3×FLAG-myc-CMV26 (Sigma) vectors were converted to destination vectors using the Gateway® vector conversion system (Invitrogen), producing pQCXIP-DEST, pQCXIH-DEST, pHcRed-DEST, and p3×FLAG-DEST, respectively. Gateway®LR reactions were performed as described in the Gateway® instruction manual (Invitrogen), to finally produce the pcDNA6.2-SMS1-V5, pcDNA6.2-SMS2-V5, pcDNA6.2-CAV1, pcDNA6.2-SMS2-EmGFP, pHcRed-CD36/FAT, pHcRed-caveolin 1, p3×FLAG-CD36/FAT, p3×FLAG-caveolin 1, pQCXIP-SMS1-V5, and pQCXIH-SMS2-V5 plasmids. All materials and reagents were of highest purity available.

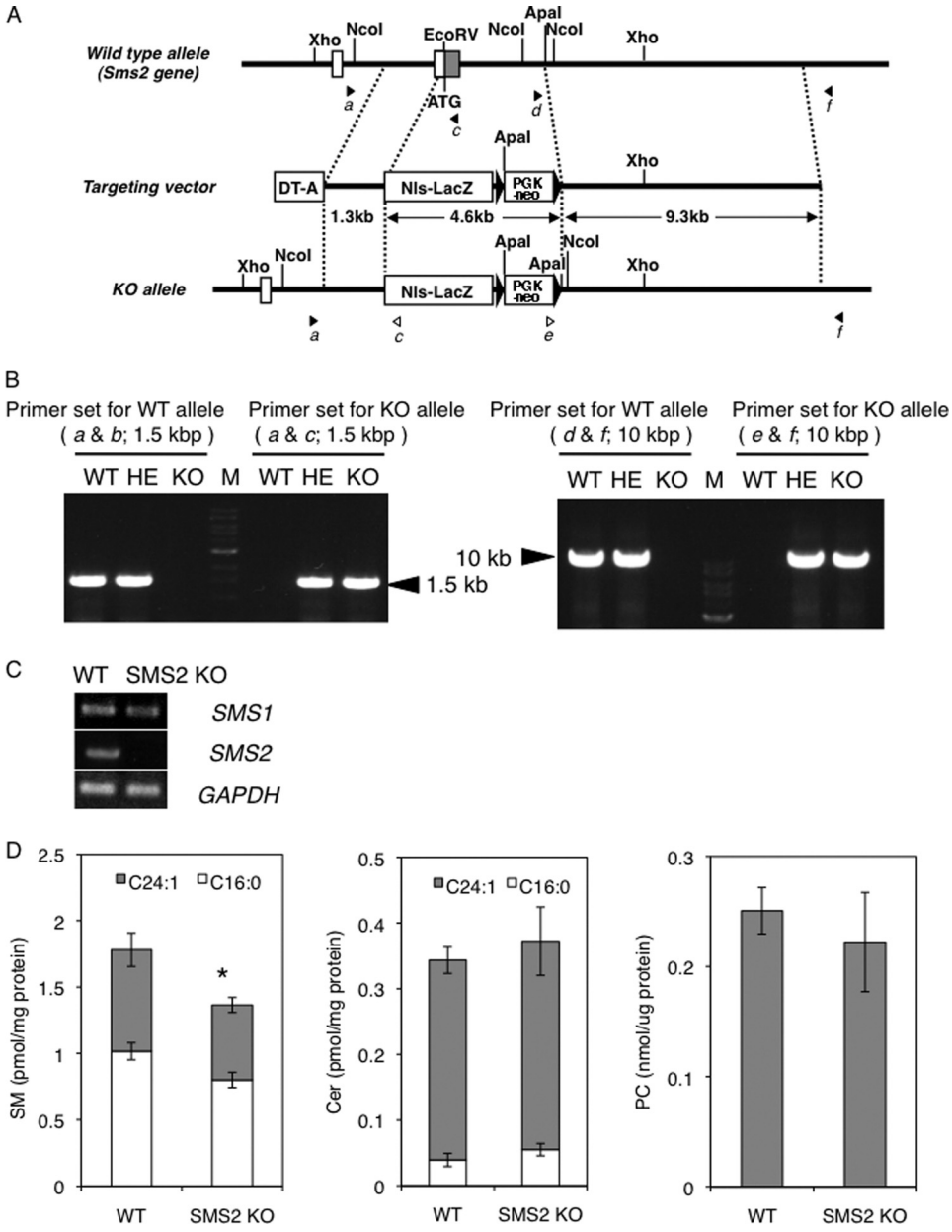

FIGURE 1. **Generation of SMS2 KO mice.** *A,* schematic of targeted disruption of SMS2. The *top* illustration is a wild type allele; the *middle* shows the targeting construct with the neomycin-resistant gene (*PGK-neo*), diphtheria toxin A chain gene (*DT-A*), and nuclear localization signal-LacZ (*NLS-LacZ*). The *bottom* illustration shows the allele mutated by homologous recombination. *Closed* and *open arrowheads* are corresponding to the primer position to detect wild type and knock-out (*KO*) alleles, respectively. *B,* confirmation of homologous recombination by long accurate-PCR using the primers indicated in *A*. The ladder is 1-kb DNA ladder (*M*). The primer sets of *a* and *b* and *d* and *f* were for WT allele; *a* and *c* and *e* and *f* were for KO allele. *HE*, heterozygote. *C,* RT-PCR was performed for the expression of SMS1, SMS2, and GAPDH in WT and SMS2 KO mice. *D,* amounts of SM, Cer, and PC were determined as described under "Experimental Procedures." Data are presented as the mean ± S.D. of five distinct mice. *, $p < 0.05$.

RESULTS

Generation of SMS2-deficient Mice—The mouse SMS2 gene (*Sgms2*) in ES cells was targeted by homologous recombination (Fig. 1*A*). The SMS2 gene was successfully disrupted (Fig. 1*B*), and this disruption was associated with a loss of SMS2 expression (Fig. 1*C*). The obtained SMS2 knock-out (SMS2 KO) mice were seemingly healthy and displayed almost no apparent abnormalities. Initially, we determined the amounts of SM, Cer, and PC in the livers of the SMS2 KO mice and control wild type (WT) mice (Fig. 1*D*). The SMS2 deficiency reduced SM levels by about 20%, with no apparent effect on Cer or PC levels. Our data indicate that most SM is synthesized by SMS1, and so the effect of SMS2 deficiency on SM levels is mild and restricted. This lack of effect on SM levels might account for the absence of abnormalities in SMS2 KO mice. These results prompted a question as to whether SMS2 might be simply redundant to SMS1. To identify a particular function of SMS2, we performed a diet-induced obesity (DIO) test.

SMS2 Deficiency Prevents High Fat Diet-induced Obesity and Insulin Resistance—In the DIO test, mice were fed a high fat diet (HFD) or normal diet (ND) from 4 to 15 weeks of age. In the wild type (WT) mice, HFD potently increased the body weight

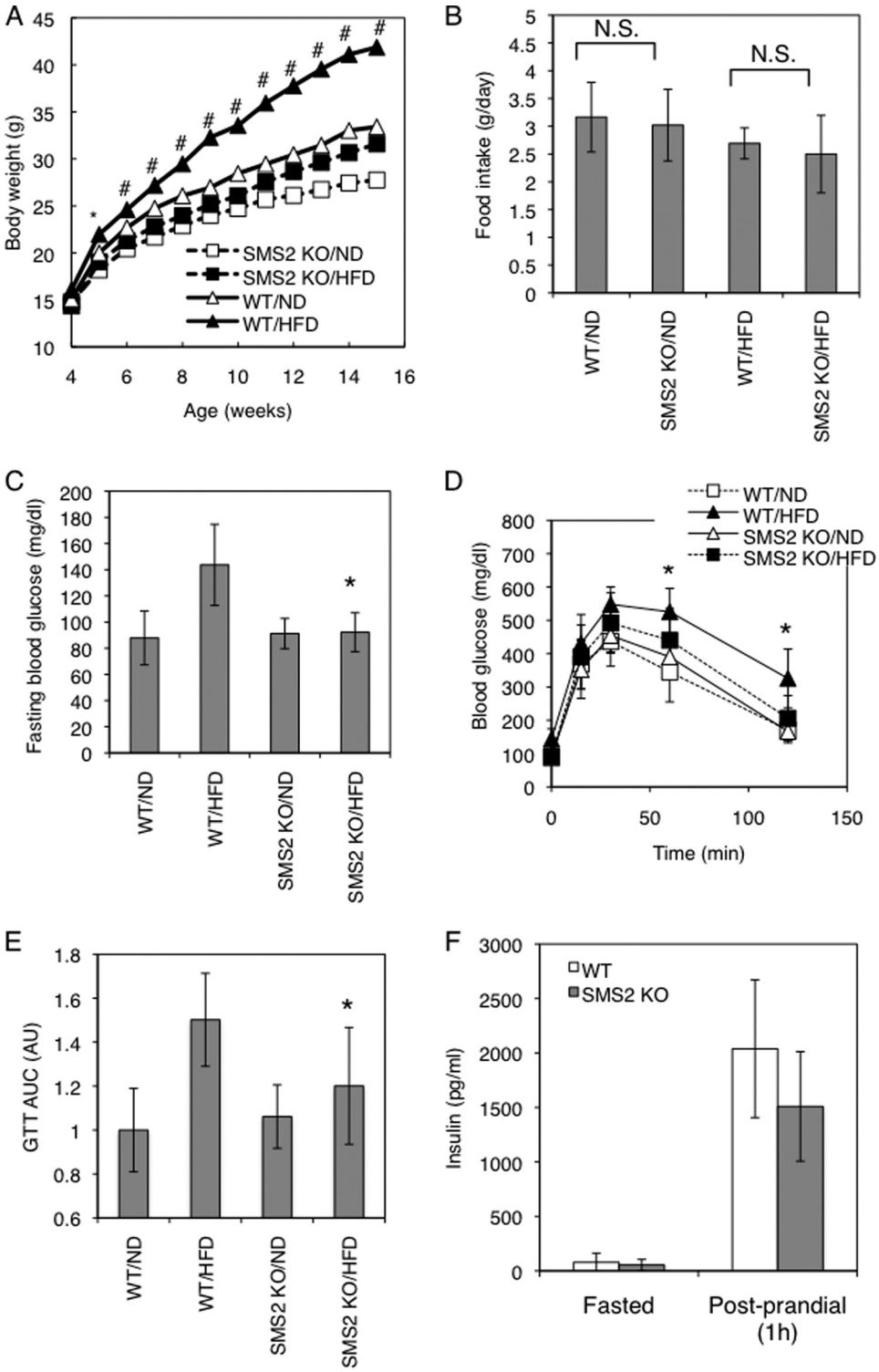

FIGURE 2. **SMS2 deficiency improves diet-induced obesity and impaired glucose tolerance.** *A,* body weight was measured in male wild type (*WT*) or SMS2 knock-out (*SMS2 KO*) mice fed a high fat diet (*HFD*) or normal diet (*ND*). $n = 15–24$ mice per group; *, $p < 0.01$; #, $p < 0.00001$ between WT/HFD and SMS2 KO/HFD. *B,* food intake was determined using both HFD-fed and ND-fed groups of WT and SMS2 KO male mice during 7–9 weeks of age. Data are presented as the mean ± S.D., using 7–8 mice. *N.S.*, not significant. *C,* fasting blood glucose was determined after an 18-h fast. *D,* GTT was performed on the mice during the DIO test. *E,* results of the GTT in *D* are expressed by the area under the curve (*AUC*). *F,* plasma insulin levels in 8-week-old male mice were determined by ELISA as under "Experimental Procedures." *C–F*, data are presented as the mean ± S.D. of experiments in 8–12 mice; *, $p < 0.05$ between WT/HFD and SMS2 KO/HFD.

(Fig. 2*A*). However, interestingly, there were no significant differences between the HFD-fed and ND-fed groups of SMS2 KO mice. The SMS2 deficiency completely prevented the HFD-induced increase in body weight. The average amounts of food intake during the DIO test were not significantly different between the SMS2 KO and WT mice (Fig. 2*B*). We also exam-

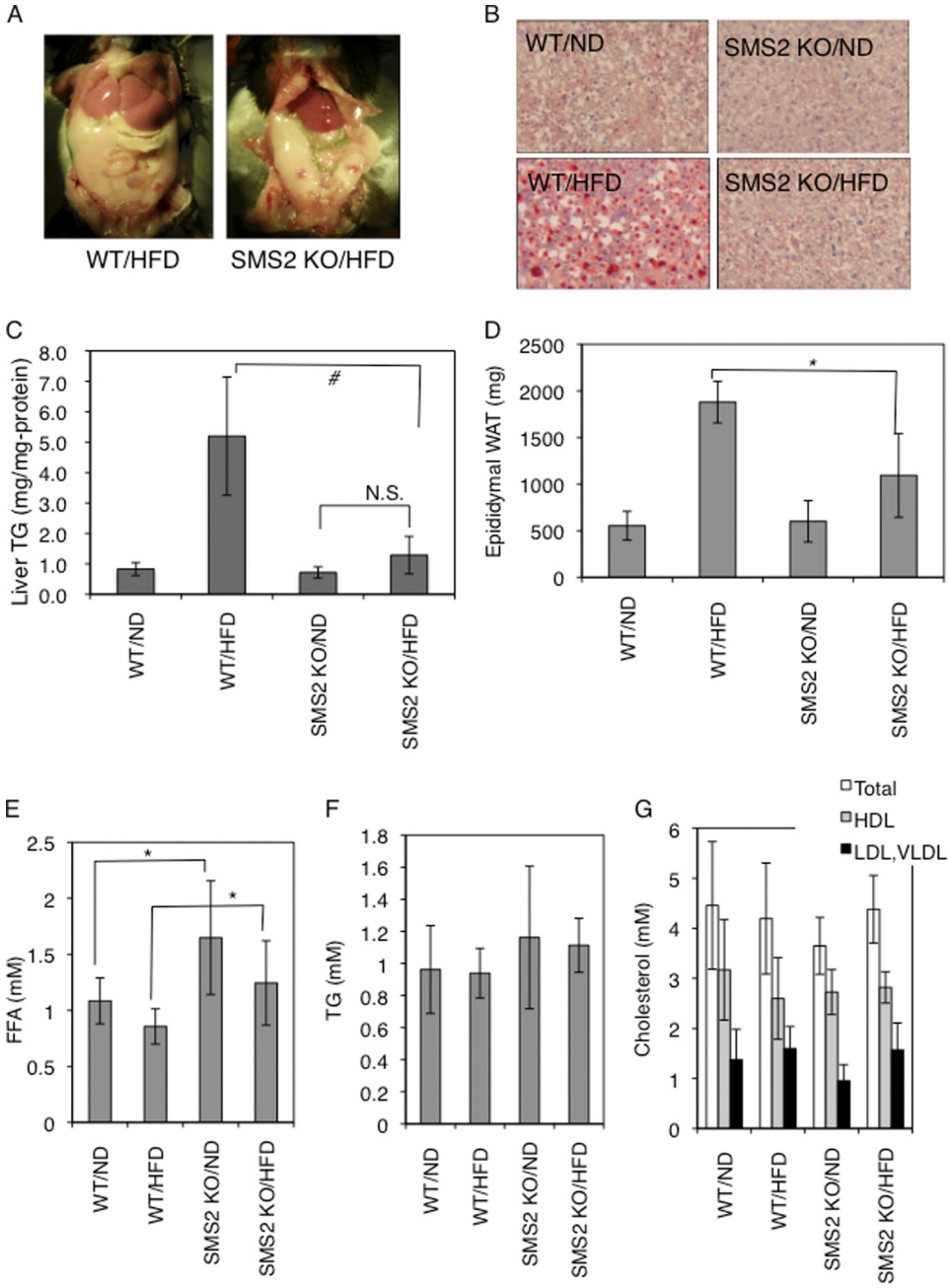

FIGURE 3. **SMS2 deficiency prevents diet-induced fatty liver formation.** *A,* after the DIO test, surgical examinations of the abdomen and liver of the mice were performed. *B,* Oil-Red-O staining was performed using frozen sections of liver. Triglyceride levels in liver (*C*), plasma levels of free fatty acid (*E*; free fatty acid (*FFA*)), triglyceride (*F*; TG), and cholesterol (*G*) were determined as described under "Experimental Procedures." *D,* amount of epididymal WAT was also measured. Data are presented as the mean ± S.D. for nine mice. *, $p < 0.05$; #, $p < 0.01$; *N.S.*, not significant.

ined the effect of SMS2 deficiency on HFD-induced glucose intolerance or insulin resistance. As expected, the fasting blood glucose was higher in the HFD-fed group of WT mice (Fig. 2*C*), indicating impaired insulin sensitivity in the liver. However, the HFD-fed group of SMS2 KO mice did not show any increase in fasting blood glucose, compared with the ND-fed group. A GTT reflected impaired blood glucose clearance in the HFD-fed group of WT mice. In contrast, the HFD-fed group of SMS2 KO mice exhibited levels of glucose clearance comparable with those of the ND-fed group of WT and SMS2 KO mice (Fig. 2, *D* and *E*). SMS1 deficiency is known to severely impair islet and insulin secretion (15), yet SMS2 KO mice were able to secrete insulin in response to feeding (Fig. 2*F*), indicating that SMS2 deficiency does not impair insulin secretion. These results show that SMS2 deficiency prevents HFD-induced insulin resistance, indicating that SMS2 is likely to be involved in the development of diabetes.

SMS2 Deficiency Prevents High Fat Diet-induced Fatty Liver—Upon surgical examination of the HFD-fed mice during the DIO test period, an impressive difference was found in the livers of WT and SMS2 KO mice. As expected, the livers of the HFD-fed WT mice grossly appeared whitish-red, indicating a fatty liver (Fig. 3*A*). Oil-Red-O staining of liver sections clearly demonstrated that the liver of HFD-fed WT mice accumulated

huge amounts of neutral lipids (red-stained spots) and large vacuous vesicles, which were the remains of large lipid droplets (Fig. 3*B*). In contrast, the livers of the HFD-fed SMS2 KO mice accumulated little or no Oil-Red-O-positive neutral lipids or large lipid droplets. The amounts of TG, a major Oil-Red-O-positive neutral lipid, were determined in these livers (Fig. 3*C*). TG levels in the HFD-fed WT mice were five times higher than those in the corresponding ND-fed group. Interestingly, no statistically significant difference was observed between the HFD-fed group and ND-fed group in SMS2 KO mice. These results clearly demonstrate that SMS2 deficiency prevents HFD-induced accumulation of TG in the liver and the resulting development of large lipid droplets and fatty liver. Additionally, the amounts of epididymal WAT were determined in each group of mice. The SMS2 deficiency clearly suppressed the growth of epididymal WAT, observed in HFD-fed WT mice (Fig. 3*D*). We also examined the levels of free fatty acid, TG, and cholesterol in plasma. There were no significant differences in plasma TG or cholesterol levels between WT and SMS2 KO mice in either the ND- or HFD-fed groups (Fig. 3, *F* and *G*). However, SMS2 KO mice exhibited higher levels of free fatty acid than WT mice did in both the HFD- and ND-fed groups (Fig. 3*E*).

To gain insight into the mechanisms of how SMS2 deficiency prevents HFD-induced obesity and fatty liver, we examined the expression levels of genes implicated in obesity and fatty liver using real time quantitative PCR in liver and adipose tissue. Interestingly, although HFD induced the expression of the fatty acid transporter CD36/FAT ~5 times in WT mice, SMS2 deficiency strongly suppressed this HFD-induced increase of CD36/FAT (Fig. 4*A*). Similar to the mRNA expression, HFD increased the protein of CD36/FAT in WT mice, yet there was almost no difference between HFD-fed and ND-fed SMS2 KO mice (Fig. 4, *C* and *D*). The nuclear receptor PPARγ, a regulator of gene expression of many lipid metabolic enzymes in response to lipid ligands such as fatty acid or its oxidized derivatives, was elevated in HFD-fed WT mice. Interestingly, the HFD-induced increase of PPARγ was also strongly suppressed in SMS2 KO mice (Fig. 4*A*). Because the expression level of CD36/FAT is elevated by PPARγ, and CD36/FAT facilitates cellular uptake of fatty acid (PPARγ ligand), their expressions are synergistically increased, leading to lipid droplet formation (29). In our WT mice, the synergistic elevations occurred in response to HFD. In contrast, the SMS2 deficiency suppressed the HFD-induced increase of CD36/FAT and PPARγ, suggesting that SMS2 could regulate CD36/FAT-mediated uptake of fatty acid. Indeed, the plasma of SMS2 KO mice possessed higher levels of free fatty acid than that of WT mice (Fig. 3*E*), also indicating impaired fatty acid uptake in SMS2 KO mice. Conversely, there were almost no differences between WT and SMS2 KO mice in either the HFD-fed groups or ND-fed groups in several genes tested (Fig. 4*A*). In the adipose tissue of WT mice, as expected, HFD decreased the expression of insulin receptor (IR), GLUT4 (major glucose transporter in adipose tissue), and adiponectin, typical symptoms of insulin resistance (Fig. 4*B*). However in SMS2 KO mice, HFD did not decrease the expression, indicating that the mice did not develop the insulin resistance. These results agree with the GTT results (Fig. 2, *D* and *E*).

SMS2 Is Involved in Large Lipid Droplet Formation in Liver—CD36/FAT on the cell surface localizes in detergent-insoluble membrane microdomains (DIM), which are rich in sphingolipids and cholesterol. Residing in DIM is important for the functions of CD36/FAT, such as the uptake of fatty acids (30). We prepared DIM fractions using CD36/FAT- and SMS2-overexpressing COS7 cells. As expected, CD36/FAT was recovered in the DIM fraction along with caveolin 1, a well known marker for DIM. A membrane-integral protein of endoplasmic reticulum, calnexin was successfully separated from the DIM fraction. Interestingly, SMS2 was also associated with the DIM fraction (Fig. 5*A*). Confocal images revealed that GFP-tagged SMS2 and HcRed-tagged CD36/FAT or HcRed-tagged caveolin 1 were co-localized in intracellular vesicular compartments of the cell (Fig. 5*B, panel a*, *yellow*, merged image). In Fig. 5*B, panel b*, CD36-HcRed and caveolin 1-HcRed also exist in plasma membrane as reported previously (31, 32). Caveolae, small intracellular invaginations of the membrane, contain many DIM and provide a platform for signal transduction and metabolism across the plasma membrane. Caveolin 1 is a major constituent of caveolae. Reportedly, caveolae-mediated endocytosis is important for cellular entry of lipids, viruses, and some nutrients; interestingly, exogenous cholesterol and glycolipids induce internalization of caveolin 1 into endosomes (31). CD36/FAT is known to promote uptake of oxLDL and fatty acid by dynamin-independent endocytosis, and exogenous oxLDL is internalized by CD36/FAT into endosomes. Serum contains oxLDL and cholesterol, so it is reasonable that both CD36/FAT and caveolin 1 are localized in intracellular vesicles, results which agree with other studies (31, 32).

To further assess the association between SMS2 and CD36/FAT, 3×FLAG-tagged CD36/FAT or 3×FLAG-tagged caveolin 1 and V5-tagged SMS2 were co-expressed in COS7 cells and then immunoprecipitation assays were performed using anti-FLAG M2 beads. SMS2 was co-precipitated with CD36/FAT (Fig. 5*C*). Additionally, SMS2 was partially co-precipitated with caveolin 1 (Fig. 5*C*).

There is recent evidence that caveolin 1 functionally interacts with CD36/FAT and regulates fatty acid uptake (33). Additionally, caveolin 1 knock-out mice exhibited impaired fatty acid uptake and lipid droplet formation (4). We examined whether knockdown of SMS2 would affect lipid droplet formation. We employed two types of siRNA, h-siSMS2-1 and h-siSMS2-2, which reduced SMS2 expression efficiently in HepG2 cells (~60% reduction in cells transfected with h-siSMS2-1 or h-siSMS2-2). The formation of lipid droplets was induced by adding oleic acid to the medium. Large and matured lipid droplets were observed in the control cells (Fig. 5*D*, *arrowheads*). Interestingly, large lipid droplets (>1.25 μm) were dramatically reduced in both SMS2 knockdown cells (Fig. 5*E*). Additionally, knockdown of SMS2 decreased the uptake of oleic acid significantly (Fig. 5*F*). These results strongly suggest that SMS2 is involved in fatty acid uptake and in the growth and maturation of lipid droplets. The data coincide with impaired lipid droplet formation in the liver of HFD-fed SMS2 KO mice (Fig. 3*E*). Critical roles for lipid microdomains in fatty acid uptake and maturation of lipid droplets have been reported (28, 34). In addition, SMS2 deficiency reportedly reduced sensi-

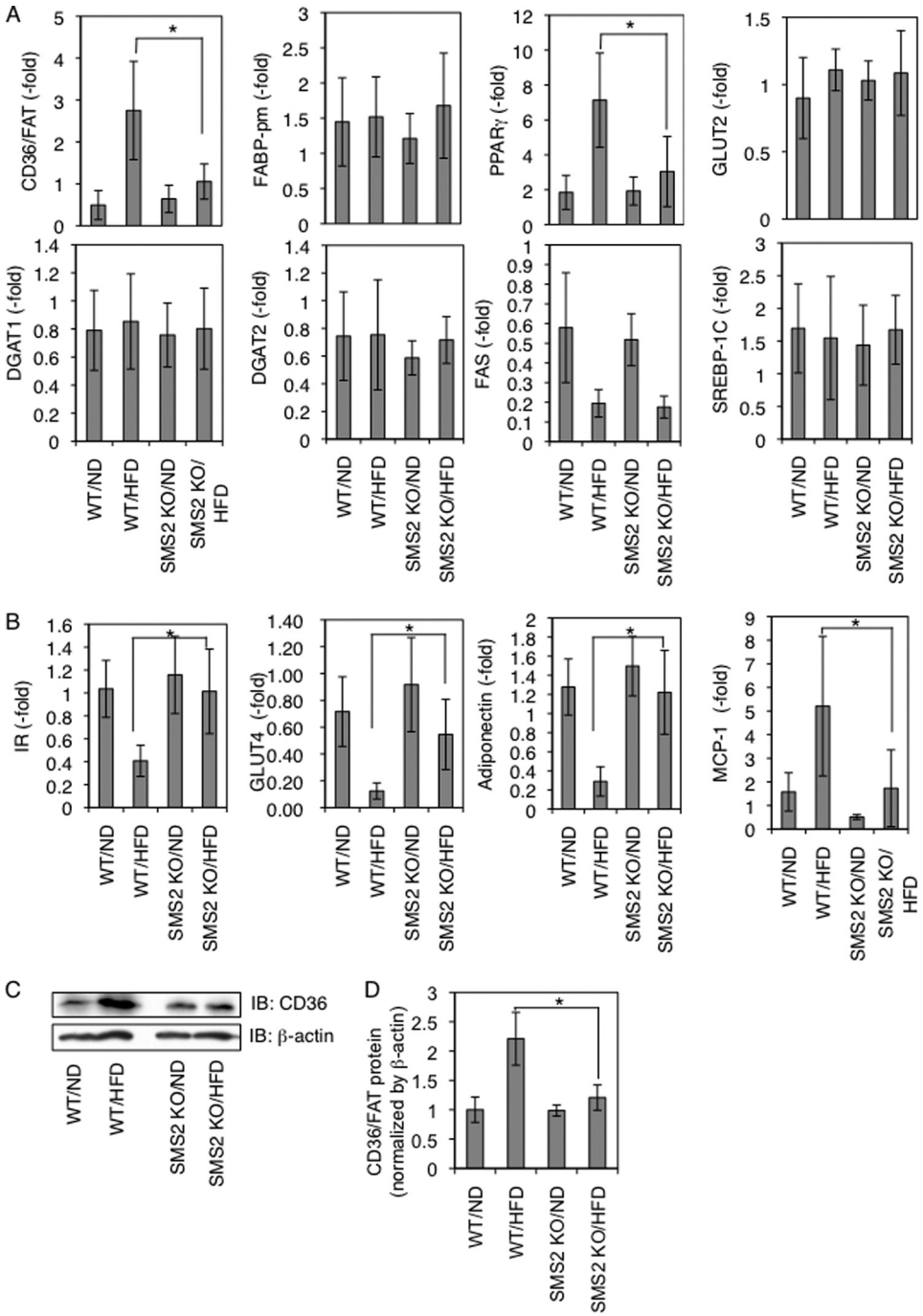

FIGURE 4. **SMS2 deficiency suppresses diet-induced elevation of CD36/FAT and PPARγ in liver.** After the DIO test, RNA was isolated from liver (*A*) and adipose tissue (*B*), and real time PCR was performed as described under "Experimental Procedures" using primers listed in supplemental Table S1. Data are presented as the mean ± S.D. for eight mice, *, $p < 0.05$. *C* and *D,* Western blotting was performed using liver lysates from each mouse, and the bands corresponding to CD36/FAT were quantified. Data are presented as the mean ± S.D. for five mice. *, $p < 0.05$. The details of the all experiments were described under "Experimental Procedures." *IB*, immunoblot.

tivity to lysenin-mediated cytolysis, indicating that SMS2 alters the lipid microdomain (35). Methyl-β-cyclodextrin (MβCD) is known to reduce cholesterol levels, disrupt lipid microdomains, and induce cell death (36). Knockdown of SMS2 clearly decreased cell viability after an overnight treatment with MβCD (Fig. 5*G*). Decreased levels of SM in lipid microdomains would increase the sensitivity of MβCD-induced cell death. These results suggest that SMS2 deficiency could cause disorder in lipid microdomains, leading to impairments in fatty acid uptake and maturation of lipid droplets. *In vivo* experiments for SMS2 knockdowns were also performed using a leptin-deficient obese model, *ob/ob* mice. with an siRNA delivery system of SNALP (24). SMS2 siRNA efficiently suppressed SMS2 expression in liver (~70% reduction in cells transfected with m-siSMS2-1 or m-siSMS2-2). Interestingly, both siRNAs of SMS2 successfully reduced TG levels in liver without changes in food intake (Fig. 5*H*).

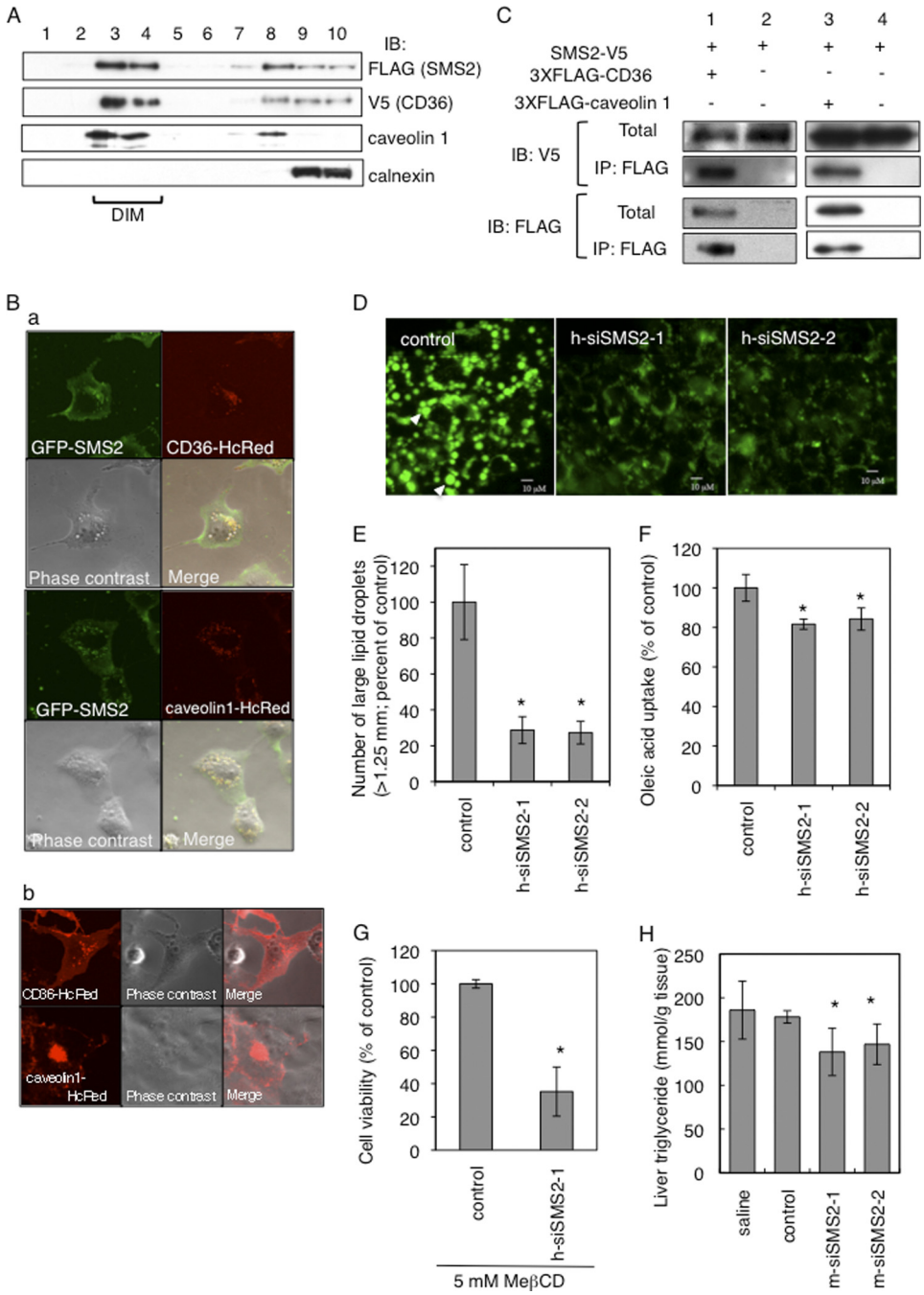

FIGURE 5. **SMS2 associates with CD36/FAT and caveolin 1 and is involved in lipid droplet formation.** *A,* FLAG-tagged SMS2 and V5-tagged CD36/FAT were co-expressed in COS7 cells, and DIM fractions were prepared, and then each protein was detected by Western blotting. *B,* confocal images of GFP-tagged SMS2 (*green*), HcRed-tagged CD36/FAT (*red*), and HcRed-tagged caveolin 1 (*red*) revealed partial co-localization of SMS2 and CD36/FAT or caveolin 1 (*panel a*; *yellow*; merged image). The COS7 cells express HcRed-Cav1 or HcReD-CD36 but do not express GFP-SMS2 (*panel b*). *C,* COS7 cells expressing SMS2-V5 and 3×FLAG-CD36/FAT or SMS2-V5 and 3×FLAG-caveolin 1 were lysed, and a co-precipitation assay was performed using anti-FLAG M2 beads. Proteins were detected by Western blotting as described under "Experimental Procedures." *IP*, immunoprecipitation; *IB*, immunoblot. *D* and *E,* after the treatment with indicated siRNA in HepG2 cells, the formation of lipid droplets was induced by adding oleic acid to the medium. Lipid droplets were stained with Nile Red (*D*), and the numbers of large lipid droplets (>1.25 μm) were counted using a fluorescent microscope (*E*). *F,* fatty acid uptake (during 10 min) was examined in HepG2 cells after the treatment with indicated siRNA. *G,* HepG2 cells were treated overnight with siRNA and then were incubated with 5 mM MβCD for 24 h. The viability of the cells was determined using a Cell Counting Kit-8 (Dojindo, Kumamoto, Japan). Data are presented as the mean ± S.D. for three independent experiments. *, $p < 0.05$ against control experiment. *H, in vivo* silencing of SMS2 in *ob/ob* mice was performed using a siRNA delivery system of SNALP. Ten days after injection of siRNA for SMS2 (m-siSMS2-1 and m-siRNA2-2), control, saline, or triglyceride levels in liver were determined. Data are presented as the mean ± S.D. for three mice. *, $p < 0.05$ against control experiment. The details of the all experiments were described under "Experimental Procedures."

SMS2 Can Convert Cer to SM at Outer Leaflet of the Plasma Membrane—To further confirm that SMS2 is involved in cellular fatty acid uptake, we isolated MEF from SMS2 knock-out mice (SMS2 KO-MEF) and control littermate WT mice (WT-MEF). We additionally produced reconstituted cells (SMS2 KO/SMS2 MEF). We then compared fatty acid uptake among these cells. The presence of SMS2 clearly elevated oleic acid uptake (Fig. 6*A*), indicating the importance of SMS2 in fatty

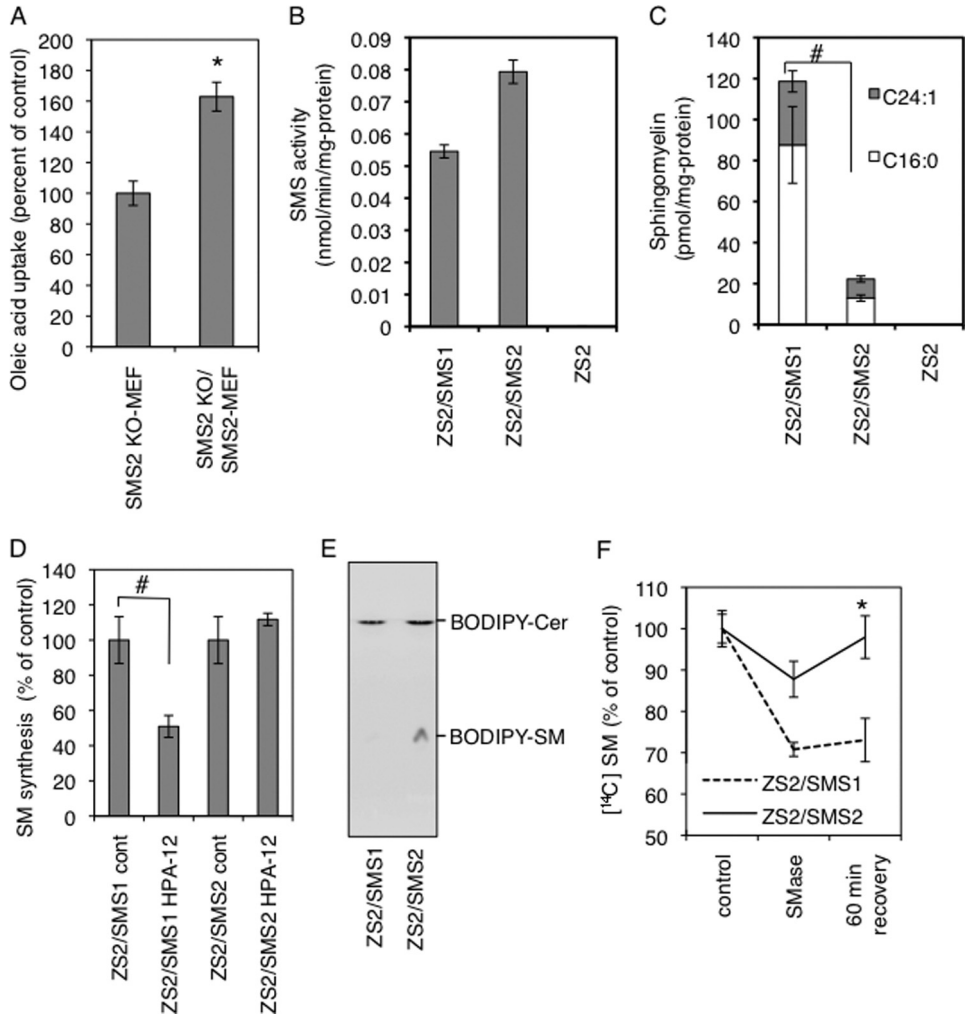

FIGURE 6. **SMS2 can convert ceramide to SM on the outer leaflet of the plasma membrane.** *A,* SMS2-deficient fibroblasts (SMS2 KO-MEF), SMS2-reconstituted fibroblasts (SMS2 KO/SMS2 MEF), and control fibroblasts (WT-MEF) were prepared as described under "Experimental Procedures," and fatty acid uptake (during 10 min) was examined. *B* and *C,* SM-reconstituted cells ZS2, ZS2/SMS1, and ZS2/SMS2 were established as described under "Experimental Procedures," and their *in vitro* sphingomyelin synthase activity (*B*) and the amount of SM (*C*) were determined. Prior to the analysis, the cells were cultured with the serum-free medium OptiPro SFM (Invitrogen) for 48 h to exclude the effect of SM supply from serum. *D,* effect of a CERT inhibitor, HPA-12, on SM synthesis in ZS2/SMS1 and ZS2/SMS2 cells was examined as described under "Experimental Procedures." *E,* cells were prelabeled with [^{14}C]choline, and the bacterial sphingomyelinase (*SMase*) was added to generate ceramide on the plasma membrane. Recovery of SM in ZS2/SMS1 and ZS2/SMS2 cells was monitored. These experiments contained dynasore, a dynamin II inhibitor, to inhibit ceramide transport from the plasma membrane to the Golgi apparatus. *A–D* and *F*, values represent the mean ± S.D. from three independent experiments. *, $p < 0.05$; #, <0.005.

acid uptake. However, it is not fully understood whether SMS2 has a function distinct from that of SMS1. To completely distinguish SMS2 function from SMS1 function, we generated a new cell line, ZS2, that lacks both SMS1 and SMS2, using mouse embryonic fibroblasts from an SMS1 and -2 double knock-out mouse. We then generated reconstituted cell lines by reintroducing the gene encoding SMS1 or SMS2, named ZS2/SMS1 or ZS2/SMS2, respectively. The ZS2 has no SM synthase activity or SM in the cell, indicating that only SMS1 and SMS2 are synthases for SM at least in mouse fibroblasts (Fig. 6, *B* and *C*). Interestingly, although SMS2 exhibits significant SM synthase activity *in vitro* (Fig. 6*B*), it contributes only one-sixth the amount of SM compared with SMS1 (Fig. 6*C*). This result indicates that Cer, a substrate of SM synthesis, is not efficiently provided to SMS2 *in vivo*. Newly synthesized Cer on endoplasmic reticulum is transferred to Golgi by the Cer transfer protein CERT, to be converted to SM (26). We examined the effect of the CERT inhibitor HPA-12 on SM synthesis in each reconstituted cell line. HPA-12 reduced SM synthesis by about half compared with controls in ZS2/SMS1, agreeing with a previous report (Fig. 6*D*) (27). However, there was no effect from HPA-12 on SM synthesis in ZS2/SMS2 cells. These results indicate that CERT-dependent SM synthesis is due to SMS1 activity and that SMS2 contributes to SM synthesis in a CERT-independent manner. The next question raised was whether SMS2 could alter from where the Cer was produced. The ZS2/SMS1 and ZS2/SMS2 cells were placed at 4 °C to stop all active transport in the cell, and the fluorescent analog of Cer, BODIPY-Cer, was added to the medium. After 30 min, rapid conversion of BODIPY-Cer to BODIPY-SM was observed in ZS2/SMS2, but not in ZS2/SMS1 cells (Fig. 6*E*), indicating the SMS2 acts on the outer leaflet of the cell, and the result agrees with previous report (37). To produce Cer on the outer leaflet of the plasma membrane, bacterial sphingomyelinase (SMase) was employed

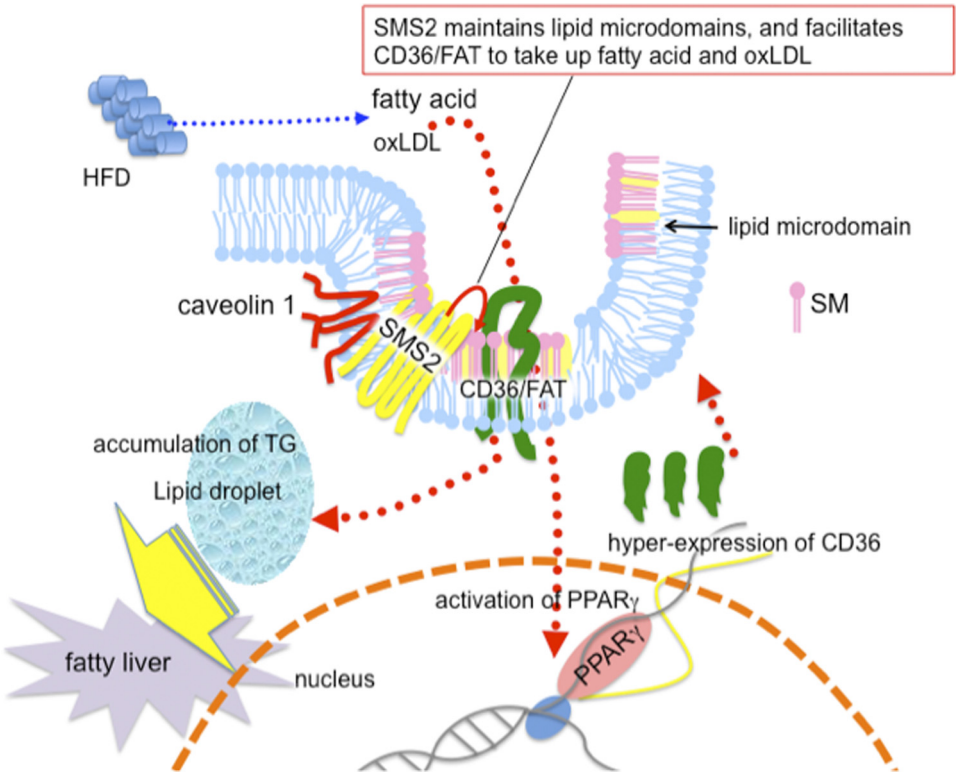

FIGURE 7. **SMS2 could be a novel regulator of lipid microdomain structure and function.** CD36/FAT is located in lipid microdomains. PPARγ is responsible for the expression of CD36/FAT. After HFD feeding, the increased fatty acid or oxLDL would be incorporated via CD36/FAT, activate PPARγ, and induce the hyper-expression of CD36/FAT, resulting in TG accumulation and fatty liver. We found that SMS2 is localized in lipid microdomains and that it associates with CD36/FAT and caveolin 1. Furthermore, we clearly demonstrated that SMS2 could convert Cer to SM on the outer leaflet of the plasma membrane. We conclude that SMS2 could be a novel regulator of lipid microdomain structure and function, and the regulation would be crucial for obesity and type 2 diabetes.

as described previously (38), and the endocytosis for recycling the produced Cer was blocked by the dynamin II inhibitor dynasore. Interestingly, in ZS2/SMS2 cells, the SM levels were reduced by SMase treatment, but 60 min after removing the SMase, the SM levels had completely recovered (Fig. 6*F*). In contrast, only moderate recovery after SMase removal was observed in ZS2/SMS1 cells. These results indicate that SMS2 could convert Cer produced at the outer leaflet of the plasma membrane to SM. Moreover, the reduction of SM levels after SMase treatment in ZS2/SMS2 cells was milder than that observed in ZS2/SMS1 cells, indicating that produced Cer will be quickly converted to SM by SMS2. These results clearly show that SMS2 can convert Cer to SM in lipid microdomains on the outer leaflet of the plasma membrane.

Altogether, SMS2 was able to regulate the dynamic structure of SM-rich lipid microdomains on the plasma membrane and could modify protein function, such as that of CD36/FAT or caveolin 1 located in the lipid microdomains. SMS2 knock-out mice exhibited disrupted regulation of the lipid microdomains function, leading to a prevention of lipid droplet formations, fatty liver, obesity, and insulin resistance.

DISCUSSION

Recent studies have revealed that exocytosis of acid sphingomyelinase by wounded cells promotes endocytosis and plasma membrane repair (39). Thus, the local elevation of Cer on the plasma membrane is important for endocytosis. It is also known that exogenously added bacterial SMase induces ATP-independent endocytosis (40). These studies suggested to us that conversion from SM to Cer causes a structural change in the plasma membrane and facilitates the formation of endocytotic vesicles. So far, the destiny of produced Cer has not been determined. In this study, we found that SMS2 could convert Cer to SM on the plasma membrane, indicating that SMS2 can modulate structural changes induced by acid sphingomyelinase on the plasma membrane. Because SM is a major component of lipid microdomains, proteins located in these microdomains would be regulated in a spatial-temporal manner by conversion of SM to Cer and reconversion of Cer to SM. Indeed, acid sphingomyelinase-deficient mice exhibited abnormal lipid microdomain formation, indicating that the conversion of SM to Cer is also necessary to maintain the homeostasis of these domains (41). Additionally, we found that SMS2 is localized in the membrane lipid microdomains and that it associates with CD36/FAT and caveolin 1 (Fig. 5, *A* and *C*). Caveolae are responsible for the uptake of lipids or nutrients via caveolae-dependent endocytosis (42), leading to the maturation of lipid droplets (43). Thus, SMS2, caveolin 1, and/or CD36/FAT might act coordinately to drive endocytosis leading to the maturation of lipid droplets. Indeed, SMS2 and CD36/FAT or caveolin 1 is co-localized in intracellular vesicular compartments of the cell (Fig. 5*B*). SMS2 would modulate the approximal lipid environment of CD36/FAT and caveolin 1 in lipid microdomains. Thus, SMS2 deficiency prevents HFD-induced fatty acid uptake and lipid droplet formation, which lead to fatty liver, obesity, and insulin resistance (Fig. 7). At this time, the functional regulation of the microdomains is thought to exclu-

sively account for the modification of proteins such as their phosphorylation, lipidation, or ubiquitinations. Our findings suggest a novel regulation system for lipid microdomains that results from the dynamic modification of lipids on the plasma membrane.

In this study, we demonstrate that SMS2 is involved in fatty liver, obesity, and type 2 diabetes. Arteriosclerosis is also reduced by SMS2 deficiency (11). We also demonstrated that *in vivo* knockdown of SMS2 improved triglyceride accumulation in the livers of *ob/ob* mice (Fig. 5*H*). SMS2 inhibitors might be one novel type of pharmaceuticals for obesity and type 2 diabetes, which would modulate lipid microdomain functions and regulate protein functions in lipid microdomains.

Acknowledgments—We are grateful to Dr. Kentaro Hanada (National Institute of Infectious Diseases, Tokyo) for kindly providing HPA12. We also thank Dr. Jinichi Inokuchi (Tohoku Pharmaceutical University, Sendai) for technical advice for the adipose research.

REFERENCES

1. Hakomori, S. I. (2000) *Glycoconj. J.* **17,** 143–151
2. Hakomori, S. I. (2010) *FEBS Lett.* **584,** 1901–1906
3. Simons, K., and Gerl, M. J. (2010) *Nat. Rev. Mol. Cell Biol.* **11,** 688–699
4. Razani, B., Combs, T. P., Wang, X. B., Frank, P. G., Park, D. S., Russell, R. G., Li, M., Tang, B., Jelicks, L. A., Scherer, P. E., and Lisanti, M. P. (2002) *J. Biol. Chem.* **277,** 8635–8647
5. Ortegren, U., Aboulaich, N., Ost, A., and Strålfors, P. (2007) *Trends Endocrinol. Metab.* **18,** 344–349
6. Yamaoka, S., Miyaji, M., Kitano, T., Umehara, H., and Okazaki, T. (2004) *J. Biol. Chem.* **279,** 18688–18693
7. Huitema, K., van den Dikkenberg, J., Brouwers, J. F., and Holthuis, J. C. (2004) *EMBO J.* **23,** 33–44
8. Tafesse, F. G., Ternes, P., and Holthuis, J. C. (2006) *J. Biol. Chem.* **281,** 29421–29425
9. Vacaru, A. M., Tafesse, F. G., Ternes, P., Kondylis, V., Hermansson, M., Brouwers, J. F., Somerharju, P., Rabouille, C., and Holthuis, J. C. (2009) *J. Cell Biol.* **185,** 1013–1027
10. Hailemariam, T. K., Huan, C., Liu, J., Li, Z., Roman, C., Kalbfeisch, M., Bui, H. H., Peake, D. A., Kuo, M. S., Cao, G., Wadgaonkar, R., and Jiang, X. C. (2008) *Arterioscler. Thromb. Vasc. Biol.* **28,** 1519–1526
11. Liu, J., Huan, C., Chakraborty, M., Zhang, H., Lu, D., Kuo, M. S., Cao, G., and Jiang, X. C. (2009) *Circ. Res.* **105,** 295–303
12. Fan, Y., Shi, F., Liu, J., Dong, J., Bui, H. H., Peake, D. A., Kuo, M. S., Cao, G., and Jiang, X. C. (2010) *Arterioscler. Thromb. Vasc. Biol.* **30,** 2114–2120
13. Hannun, Y. A., and Obeid, L. M. (2008) *Nat. Rev. Mol. Cell Biol.* **9,** 139–150
14. Kim, R. H., Takabe, K., Milstien, S., and Spiegel, S. (2009) *Biochim. Biophys. Acta* **1791,** 692–696
15. Yano, M., Watanabe, K., Yamamoto, T., Ikeda, K., Senokuchi, T., Lu, M., Kadomatsu, T., Tsukano, H., Ikawa, M., Okabe, M., Yamaoka, S., Okazaki, T., Umehara, H., Gotoh, T., Song, W. J., Node, K., Taguchi, R., Yamagata, K., and Oike, Y. (2011) *J. Biol. Chem.* **286,** 3992–4002
16. Mitsutake, S., Yokose, U., Kato, M., Matsuoka, I., Yoo, J. M., Kim, T. J., Yoo, H. S., Fujimoto, K., Ando, Y., Sugiura, M., Kohama, T., and Igarashi, Y. (2007) *Biochem. Biophys. Res. Commun.* **363,** 519–524
17. Dentin, R., Benhamed, F., Hainault, I., Fauveau, V., Foufelle, F., Dyck, J. R., Girard, J., and Postic, C. (2006) *Diabetes* **55,** 2159–2170
18. Ohno, Y., Suto, S., Yamanaka, M., Mizutani, Y., Mitsutake, S., Igarashi, Y., Sassa, T., and Kihara, A. (2010) *Proc. Natl. Acad. Sci. U.S.A.* **107,** 18439–18444
19. Houjou, T., Yamatani, K., Nakanishi, H., Imagawa, M., Shimizu, T., and Taguchi, R. (2004) *Rapid Commun. Mass Spectrom.* **18,** 3123–3130
20. Takagi, S., Tojo, H., Tomita, S., Sano, S., Itami, S., Hara, M., Inoue, S., Horie, K., Kondoh, G., Hosokawa, K., Gonzalez, F. J., and Takeda, J. (2003) *J. Clin. Invest.* **112,** 1372–1382
21. Laemmli, U. K. (1970) *Nature* **227,** 680–685
22. Towbin, H., Staehelin, T., and Gordon, J. (1979) *Proc. Natl. Acad. Sci. U.S.A.* **76,** 4350–4354
23. Pohl, J., Ring, A., Korkmaz, U., Ehehalt, R., and Stremmel, W. (2005) *Mol. Biol. Cell* **16,** 24–31
24. Semple, S. C., Akinc, A., Chen, J., Sandhu, A. P., Mui, B. L., Cho, C. K., Sah, D. W., Stebbing, D., Crosley, E. J., Yaworski, E., Hafez, I. M., Dorkin, J. R., Qin, J., Lam, K., Rajeev, K. G., Wong, K. F., Jeffs, L. B., Nechev, L., Eisenhardt, M. L., Jayaraman, M., Kazem, M., Maier, M. A., Srinivasulu, M., Weinstein, M. J., Chen, Q., Alvarez, R., Barros, S. A., De, S., Klimuk, S. K., Borland, T., Kosovrasti, V., Cantley, W. L., Tam, Y. K., Manoharan, M., Ciufolini, M. A., Tracy, M. A., de Fougerolles, A., MacLachlan, I., Cullis, P. R., Madden, T. D., and Hope, M. J. (2010) *Nat. Biotechnol.* **28,** 172–176
25. Mitsutake, S., Suzuki, C., Akiyama, M., Tsuji, K., Yanagi, T., Shimizu, H., and Igarashi, Y. (2010) *J. Dermatol. Sci.* **60,** 128–129
26. Hanada, K., Kumagai, K., Yasuda, S., Miura, Y., Kawano, M., Fukasawa, M., and Nishijima, M. (2003) *Nature* **426,** 803–809
27. Yasuda, S., Kitagawa, H., Ueno, M., Ishitani, H., Fukasawa, M., Nishijima, M., Kobayashi, S., and Hanada, K. (2001) *J. Biol. Chem.* **276,** 43994–44002
28. Pohl, J., Ring, A., Ehehalt, R., Schulze-Bergkamen, H., Schad, A., Verkade, P., and Stremmel, W. (2004) *Biochemistry* **43,** 4179–4187
29. Nagy, L., Tontonoz, P., Alvarez, J. G., Chen, H., and Evans, R. M. (1998) *Cell* **93,** 229–240
30. Ehehalt, R., Sparla, R., Kulaksiz, H., Herrmann, T., Füllekrug, J., and Stremmel, W. (2008) *BMC Cell Biol.* **9,** 45
31. Singh, R. D., Puri, V., Valiyaveettil, J. T., Marks, D. L., Bittman, R., and Pagano, R. E. (2003) *Mol. Biol. Cell* **14,** 3254–3265
32. Fujimoto, T., Kogo, H., Nomura, R., and Une, T. (2000) *J. Cell Sci.* **113,** 3509–3517
33. Ring, A., Le Lay, S., Pohl, J., Verkade, P., and Stremmel, W. (2006) *Biochim. Biophys. Acta* **1761,** 416–423
34. Fernández, M. A., Albor, C., Ingelmo-Torres, M., Nixon, S. J., Ferguson, C., Kurzchalia, T., Tebar, F., Enrich, C., Parton, R. G., and Pol, A. (2006) *Science* **313,** 1628–1632
35. Liu, J., Zhang, H., Li, Z., Hailemariam, T. K., Chakraborty, M., Jiang, K., Qiu, D., Bui, H. H., Peake, D. A., Kuo, M. S., Wadgaonkar, R., Cao, G., and Jiang, X. C. (2009) *Arterioscler. Thromb. Vasc. Biol.* **29,** 850–856
36. Fukasawa, M., Nishijima, M., Itabe, H., Takano, T., and Hanada, K. (2000) *J. Biol. Chem.* **275,** 34028–34034
37. Ternes, P., Brouwers, J. F., van den Dikkenberg, J., and Holthuis, J. C. (2009) *J. Lipid Res.* **50,** 2270–2277
38. Mitsutake, S., and Igarashi, Y. (2007) *Biochem. Biophys. Res. Commun.* **359,** 622–627
39. Tam, C., Idone, V., Devlin, C., Fernandes, M. C., Flannery, A., He, X., Schuchman, E., Tabas, I., and Andrews, N. W. (2010) *J. Cell Biol.* **189,** 1027–1038
40. Zha, X., Pierini, L. M., Leopold, P. L., Skiba, P. J., Tabas, I., and Maxfield, F. R. (1998) *J. Cell Biol.* **140,** 39–47
41. Otterbach, B., and Stoffel, W. (1995) *Cell* **81,** 1053–1061
42. Doherty, G. J., and McMahon, H. T. (2009) *Annu. Rev. Biochem.* **78,** 857–902
43. Farese, R. V., Jr., and Walther, T. C. (2009) *Cell* **139,** 855–860